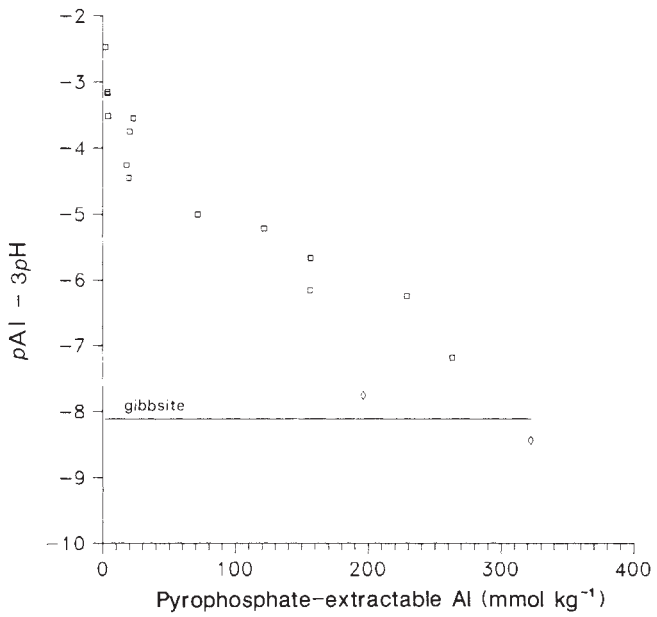

Fig. 3 Values for $p\mathrm{Al} - 3p\mathrm{H}$ in equilibrium leachates as a function of $Na_4P_2O_7$-extractable aluminium. Leachates are from all soil samples after 10, 25 and 50 HCl additions (squares). For the samples of the two podzol Bhs horizons values of the first leachate are also given (diamonds). Aluminium activities were calculated using the chemical equilibrium program ALCHEMI (ref. 18). For gibbsite we used $pK = -8.11$ (ref. 13).

introduction of acid rain produces a drastic change in the naturally occurring podzolization process.

The mobility of aluminium in the Hubbard Brook soils is significantly lower than in the Dutch soils (Table 1), because of higher soil-solution *p*H values, which is due, in turn, to a lower acid load and higher mobilization rates of base cations[15].

The current rapid depletion of organic aluminium in the rooting zone of many acid, sandy soils is irreversible on a timescale of decades or centuries. Because aqueous aluminium concentrations are in equilibrium with solid-phase alumino-organics, depletion upon continued acid deposition will inevitably lead to a reduction in dissolved aluminium concentrations. At the same time, soil-solution *p*H values, which are currently buffered in the *p*H range 3.5–4.2 by dissolution of aluminium[3] (J.M. *et al.*, preprint), may drop to values just below 3. Such dramatic changes in the soil solution chemistry of the rooting zone may have significant ecological consequences. Therefore, depletion of solid-phase organic aluminium and the associated changes in the chemical composition of soil solutions should be incorporated in current soil-acidification models.

We thank the Dutch State Forest Service and Mr W. A. M. Rijken for making available the research sites. This study was supported in part by the EEC and by the Netherlands Technology Foundation (STW).

Received 11 August; accepted 22 November 1988.

1. Van Breemen, N., Driscoll, C. T. & Mulder, J. *Nature* **307**, 599–604 (1984).
2. Khanna, P. K., Prenzel, J., Meiwes, K. J., Ulrich, B. & Matzner, E. *Soil Sci. Soc. Am. J.* **51**, 446–452 (1987).
3. Mulder, J., van Grinsven, J. J. M. & van Breemen, N. *Soil Sci. Soc. Am. J.* **51**, 1640–1646 (1987).
4. Andersson, F. & Kelly, J. M. (eds) *Aluminium Toxicity to Trees* (Swedish University of Agricultural Sciences, Uppsala, Sweden, 1984).
5. Pavan, M. H. & Bingham, F. T. *Soil Sci. Soc. Am. J.* **46**, 993–997 (1982).
6. Wright, R. J., Baligar, V. C. & Wright, S. F. *Soil Sci.* **144**, 224–232 (1987).
7. Ulrich, B., Mayer, R. & Khanna, P. K. *Soil Sci.* **130**, 193–199 (1980).
8. Richburg, J. S. & Adams, F. *Soil Sci. Soc. Am. Proc.* **34**, 728–734 (1970).
9. Bloom, P. R., McBride, M. B. & Weaver, R. M. *Soil Sci. Soc. Am. J.* **43**, 488–493 (1979).
10. David, M. B. & Driscoll, C. T. *Geoderma* **33**, 297–318 (1984).
11. Driscoll, C. T., van Breemen, N. & Mulder, J. *Soil Sci. Soc. Am. J.* **49**, 437–444 (1985).
12. Cronan, C. S., Walker, W. J. & Bloom, P. R. *Nature* **324**, 140–143 (1986).
13. May, H. M., Helmke, P. A. & Jackson, M. L. *Geochim. cosmochim. Acta* **43**, 861–868 (1979).
14. Kamprath, E. J. *Soil Sci. Soc. Am. Proc.* **34**, 352–354 (1970).
15. Mulder, J. & van Breemen, N. in *Effects of Atmospheric Pollutants on Forests, Wetlands and Agricultural Ecosystems* (eds Hutchinson, T. C. & Meema, K. M.) 361–376 (Springer, Berlin, 1987).
16. USDA *Soil Survey Laboratory Methods and Procedures for Collecting Soil Samples* (USDA, Washington DC, 1972).
17. Parfitt, R. L. & Childs, C. W. *Aust. J. Soil Res.* **26**, 121–144 (1988).
18. Schecher, D. W. & Driscoll, C. T. *Wat. Resour. Res.* **23**, 525–534 (1987).

A new picture of the Moho under the western Alps

ECORS–CROP Deep Seismic Sounding Group*

The Moho—the boundary between crust and mantle first discovered by A. Mohorovicic[1]—is the main seismic marker in the continental lithosphere. The seismic nature of this interface, in terms of its position, topography, smoothness and continuity, may preserve imprints of the regional geodynamic evolution of the lithosphere. Here we report the results of a wide-angle seismic profiling experiment across the western Alps, which allows us to draw a cross-section of the Moho across this mountain belt. A tight sampling of this deep reflector shows abrupt changes in its depth and dip. The root zone of the chain (the zone of maximum crustal thickness) is well defined, with a 55-km-deep crust–mantle boundary. The Moho under the western Po plain is also clearly seen, and a shallow reflective structure is mapped under the Briançonnais zone in the 25–30 km depth range. This structure, if interpreted as lower-crustal or upper-mantle material, would support the hypothesis of a flaking of the lithosphere under the western Alps[2,3].

To prepare the layout of the vertical reflection line through the western Alps that formed the basis of the ECORS–CROP project[4,5] in 1986, a preliminary series of experiments[6] was conducted which aimed at mapping very deep interfaces along a cross-section extending from Grenoble (France) to the Po Plain (Italy). One-ton charges were detonated at five places (Fig. 1) and part of the recording array—low-frequency geophones and autonomous recorders—was deployed along fan profiles, a method which had already proved successful in other orogenic belts[7–9]. The fan radii were chosen so as to coincide with the theoretical maximum amplitude of reflections, corresponding to total reflection, at and beyond a critical distance. The Moho depth was assumed to be ~40 km, with an increase from west to east; the fan radii therefore ranged from 90 to 130 km. Because the velocity is assumed to be constant within the crust, and because each shot-station line is along the local strike of the Alps, no apparent dip of the reflector is expected. Each mirror point (triangles in Fig. 1) can therefore be plotted half-way between the shot-point and the station. With an average station spacing of 4 km along the fans, the reflectors are thus sampled every 2 km.

The fan data were processed to construct two composite cross-sections of the Alpine chain, showing the topography of deep reflectors (Figs 2 and 3). Figure 2*a*, corresponding to shots A, B and C, begins 30 km west of the Belledonne External Crystalline Massif (ECM) and extends through the Briançonnais and Piedmontese zones to the east of the Dora Maira Internal Crystalline Massif (ICM); Fig. 2*b* (shots D and LW) extends from the Gran Paradiso ICM to the Po Plain, intersecting the Sesia–Lanzo zone and the Canavese line, which marks the western limit of the chain. It should be understood that these

* A. Hirn & S. Nadir, Institut de Physique du Globe, 4 place Jussieu, Paris, France; F. Thouvenot, Laboratoire de Géophysique Interne et Tectonophysique, Observatoire de Grenoble, IRIGM, 38041 Grenoble, France (contact address); R. Nicolich & G. Pellis, Istituto di Miniere e Geofisica Applicata, Università di Trieste, I-34127 Trieste, Italy; S. Scarascia & I. Tabacco, Istituto di Geofisica della Litosfera and Istituto Fisica Terrestre, Milano, Italy; F. Castellano, Osservatorio Vesuviano, Napoli, Italy; F. Merlanti, Istituto di Geofisica, Università di Genova, Italy.

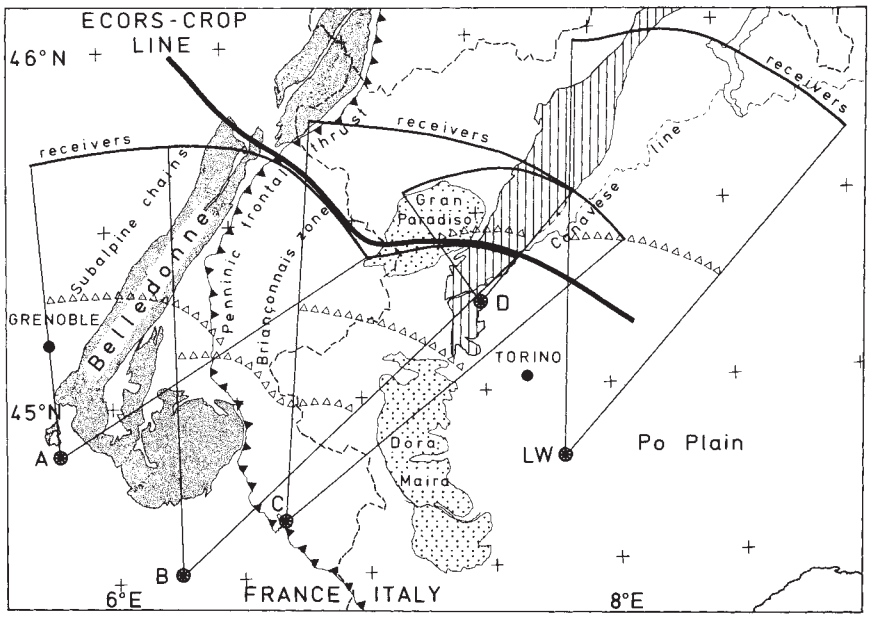

Fig. 1 Position map of the fan layout, showing the 5 shot-points A, B, C, D and LW. Open triangles indicate reflection points used to construct Fig. 2. Shaded area represents external crystalline massifs; dotted area represents internal crystalline massifs; hatched area represents the Sesia–Lanzo unit.

cross-sections combine fans with unavoidable offsets between them; for example, in Fig. 1, mirror points for shot D are shifted northwards by about 50 km relative to those for shot B. For this reason we chose to separate the two northern fans (D and LW) from the three southern ones, to keep a minimum of continuity within a composite cross-section. According to the Bouguer gravity map[10], the deep structures can be assumed to retain a cylindrical geometry for at least the 30-km extension across the section considered here.

On the seismic sections, reflections are picked using a maximum-amplitude criterion together with a correlation between traces. Around the critical distance, the wavelet reflected from the Moho is known to be very energetic, so that it can be identified with the maximum-amplitude signal. The sharpness of the onset of the reflected wavelet varies throughout the section (compare, for example, the two ends of the section in Fig. 2*a*), probably because of a variation in the seismic response of the reflector. Large (~20-km) variations in depth of the Moho marker are evident, and dips reaching 20° and extending over distances of tens of kilometres are observed. In the ECM area (Figs 2*a* and 3), the changes in depth and dip do not occur smoothly, as if by continuous flexure: from being almost horizontal at a depth of 37 km under the sub-alpine massifs and the ECMs, the Moho dips abruptly from 37 km to 55 km at their eastern edge, where the present-day maximum surface relief is found. Towards the innermost parts, under the Piedmontese zone and the Dora Maira ICM, it remains at a more or less constant, deep level of 55 km. The conversion of reflection times to depths depends on the mean crustal velocity, which is here taken to have the value 6.25 km s^{-1}; from previous seismic experiments[11–15], this value is known to be rather constant over this region so that we can assume that the depths thus obtained are accurate to better than 5%.

This deep Moho is overlaid by another seismic marker with high reflectivity (Fig. 2*a*, shot C). The maximum amplitude of the signals from the latter occur at depths of between 25 and 30 km, although it is difficult to determine accurate arrival times for these. Common experience in deep seismic profiling suggests that this reflective zone should be associated with a velocity contrast of more than 1 km s^{-1}, so that it corresponds either to the top of lower-crustal material or to a crust-mantle boundary. Situated at shallow depth and extending westwards beneath the Piedmontese zone and the ICMs as far as the Briançonnais zone, this reflector can be detected only when shooting from C. It acts as a mask which prevents the seismic energy from penetrating deeper, so that from shot-point C no deep Moho

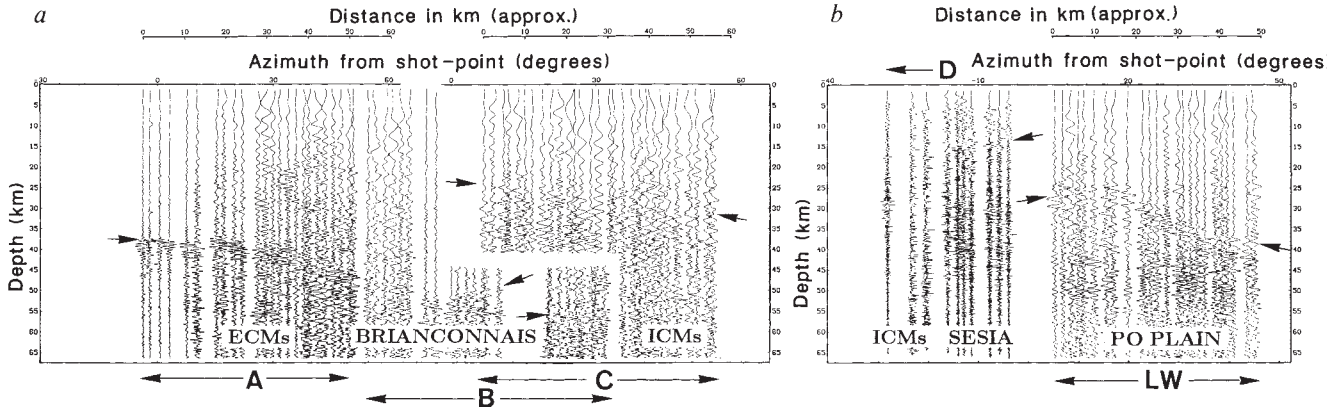

Fig. 2 Two composite cross-sections of the western Alps. *a*, The three fan profiles from shot-points A, B and C (see position on Fig. 1) are combined as a single record-section extending from the Chartreuse sub-alpine massif (far left) to the Dora Maira massif (far right). *b*, This shorter section combines results from shot-points D and LW and extends from the Gran Paradiso massif (far left) to the Po plain (far right). In each trace, the maximum-amplitude signal corresponds to reflection from the Moho. Earlier (shallower) energy arrivals may be ascribed to intracrustal discontinuities. For shot D, recorded at the relatively short distance of 40 km, the late (deep) arrivals are principally transverse S waves rather than reflected waves. Depths are calculated assuming a mean crustal velocity of 6.25 km s^{-1}.

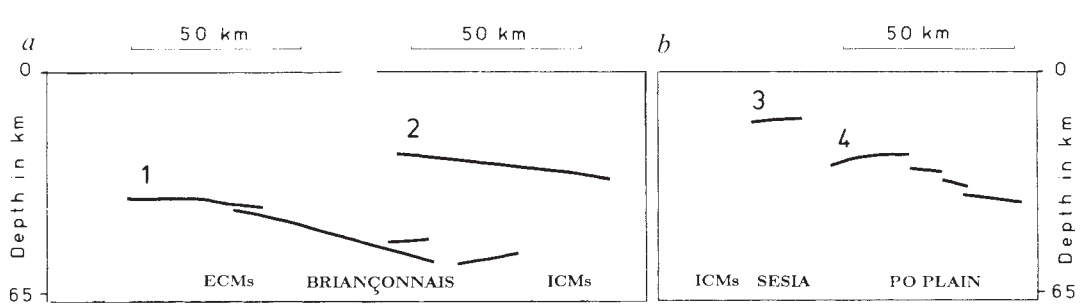

Fig. 3 Schematic line drawings of the profiles revealed by the corresponding seismograms in Fig. 2. (1) Autochthonous deep Moho; (2) Briançonnais reflector; (3) Ivrea body reflector; (4) hinterland (Po plain) Moho. In lithospheric flaking optics, features (2) and (3) trace the imbrication of anomalous upper mantle within the Alpine pile.

could be mapped. From shot-points A or B, however, the deep Moho can be reached, illustrating both the limited extent of this shallow unit and the importance of the shot/recording-array geometry in detecting such a feature.

The hinterland Moho (Fig. 2*b*), more than 35 km deep under the Po plain, where thick Tertiary–Quaternary sequences occur, seems to rise in a stepwise fashion to less than 25 km approaching the Canavese fault zone. Across this zone, there exists a gap in the seismic data, so that one cannot rule out the existence of another uprising of material with high seismic velocities. The Sesia zone is underlain by a strong reflector at a depth of only 13 km, which may correspond to a crust–mantle boundary. However, other deep reflectors in the same area, seen along a complementary longitudinal profile through Sesia, cast doubt on whether the hinterland Moho extends this far west and at such shallow depth; in a zone close to the Lanzo massif, where slices of lower-crustal and upper-mantle material have been brought up to the surface, reflective levels might be rather discontinuous. Nevertheless, the simplest structural scheme is to link the 13-km deep reflector discovered under the Sesia zone to the Po plain Moho further east.

From this wide-angle reflection profiling therefore emerges the first detailed picture of the geometry of the Moho beneath the Alps, incorporating even the innermost zones. Previous experiments[11–15] sampled the Moho too sporadically so that only smooth variations could be mapped. Close-ups of the sections presented here show that such a continuous geometry is not entirely correct, as was previously suggested by a teleseismic prospecting of lithospheric contrasts beneath the Alps[16]. This conclusion results mainly from the high spatial resolution made available by the arrangement of the fans, which provided a 2-km sampling interval of reflectors along the cross-sections.

The shallow reflective level that we have discovered under the Briançonnais zone has never before been mapped, although recently published models of Alpine orogenesis[2] have suggested such a feature. The presence of lower-crustal or upper-mantle material would indicate a tectonic thickening, resulting from previously adjacent eastern lithospheric segments having been thrust onto the western segment (the alternative, internal deformation of the sole crust, is unlikely). This would suggest flaking of the European lithosphere under the western Alps, which is discussed more thoroughly elsewhere[5].

The Ivrea body, an anomalously shallow mantle unit discovered from gravity evidence in early geophysical experiments in the Alps[11], is sampled here from shot-point D, but our experiment is unable to define its exact geometry. It is much too shallow (13 km depth) to be connected directly to the Briançonnais reflector, 30 km under the ICMs. The anomalous upper mantle imbricated within the Alpine crust therefore consists of two distinct units, the Ivrea body and the new unit discovered here.

The fan layout of the experiment proved successful in detecting very deep reflections, and the ECORS–CROP vertical reflection line was able to provide information on upper- and mid-crustal reflectors. Uniting vertical reflection profiling with the more versatile wide-angle reflection method therefore provides the sort of complementary information required to determine the deep structure of such complex orogens as the Alpine chain.

This reconnaissance project was funded by the ECORS (France) and CROP (Italy) national programmes. The participation of numerous field operators, as well as the support and willingness of local authorities at the shot-points, are acknowledged. We thank L. Jenatton for help with the artwork.

Received 6 June; accepted 29 November 1988.

1. Mohorovicic, A. *Jb. Met. Obs. Agram.* **9**, 1–63 (1909).
2. Ménard, G. & Thouvenot, F. *Bull. Soc. géol. Fr.* **5**, 147–156 (1984).
3. Butler, R. W. H. *J. geol. Soc. Lond.* **143**, 857–873 (1986).
4. Bayer, R. *et al. C. R. Acad. Sci. Paris* **305**, 1461–1470 (1987).
5. ECORS-CROP Working Group (in preparation).
6. ECORS-CROP Deep Seismic Sounding Group, *Tectonophysics* (submitted).
7. Hirn, A. *et al. Geophys. Res. Lett.* **7**, 263–266 (1980).
8. Hirn, A. *et al. Nature* **307**, 23–25 (1984).
9. Hirn, A. *et al. Ann. Geophys.* **2**, 113–117 (1984).
10. Bayer, R. & Lanza, R. *Tectonophysics* (submitted).
11. Closs, H. & Labrouste, Y. *Mém. Coll. CNRS Paris, Ann. Géophys. Int.* **XII-2**, 241 (1963).
12. Choudhury, M., Giese, P. & de Visintini, G. *Boll. Geofis. teor. appl.* **XII/51–52**, 211–240 (1971).
13. Perrier, G. thesis, Univ. Paris (1973).
14. Giese, P. & Prodehl, C. *Explosion Seismology in Central Europe* (Springer, Heidelberg, 1976).
15. Miller, H., Müller, St. & Perrier, G. *Alpine Mediterranean Geodynamics, Am. Geophys. Un. Geodyn. Ser.* **7**, 175–203 (1982).
16. Hirn, A. *et al. Nature* **308**, 531–532 (1984).

Testing the completeness of earthquake catalogues and the hypothesis of self-similarity

Paul A. Rydelek & I. Selwyn Sacks

Department of Terrestrial Magnetism, Carnegie Institution of Washington, 5241 Broad Branch Road N.W., Washington, DC 20015, USA

Self-similarity of the earthquake process is consistent with the observed linear *b*-value relation $\log(N) = a - bM$, where N is the number of earthquakes with magnitude M. Deviations from linearity are believed to be due to statistical fluctuations because of the scarcity of events at large M, or from incompleteness because of a detection threshold at small M. Above some magnitude level, all local events are detected, because they exceed the noise background on the seismogram. As magnitude decreases, however, events go undetected as the seismic signal approaches the noise background. Thus more of the smallest events should be logged at night than during the day, because the cultural noise sources and winds are diminished at night, resulting in presumably quieter seismograms. Here we use this day-to-night noise modulation to develop a completeness test for earthquake catalogues; catalogues that indicate no significant modulation are considered complete. We test three catalogues and show that the completeness magnitude can be different from the magnitude at which the *b*-value departs from linearity. In particular, catalogues that show significant deviations in linearity at small M but are otherwise complete, are at odds with the hypothesis of earthquake self-similarity.